Journal of
Ceramic Science
and Technology

J. Ceram. Sci. Technol., **09** [1] 61-68 (2018)
DOI: 10.4416/JCST2017-00076
available online at: http://www.ceramic-science.com

Effects of Growth Rate on Microstructure and Properties of Directionally Solidified Eutectic Ceramic $Al_2O_3/MgAl_2O_4/ZrO_2$

Z. Chu[1, 2], S. Wang[1, 2], J. Liu*[1, 2], J. Wang[1, 2]

[1]School of Material Science and Engineering, Shandong University of Technology, Zibo 255049, China
[2]National Engineering Research Center of Industrial Ceramics of China, 12 Zhangzhou Road, Zibo 255049, China

received September 18, 2017; received in revised form November 23, 2017; accepted Januar 9, 2018

Abstract

Directionally solidified $Al_2O_3/MgAl_2O_4/ZrO_2$ ternary eutectic ceramic was prepared by means of induction heating zone melting (IHZM), and the effects of the growth rate on the microstructure and properties of the solidified ceramic were investigated. X-ray diffraction (XRD) patterns showed that the eutectic rod contained Al_2O_3, $MgAl_2O_4$ and ZrO_2 phases. The results of scanning electron microscopy (SEM) and energy-dispersive spectroscopy (EDS) demonstrated that $Al_2O_3/MgAl_2O_4$ constituted the matrix of the eutectic ceramic while rod-like ZrO_2 was uniformly embedded in the matrix. The specimen morphology is transformed from an irregular pattern to a regular bar-shaped pattern with the increase in the growth rate. The measured and calculated value of $\lambda^2 v$ (λ, the phase spacing; v, the solidification rate) was approximately equal to 2.98, which fitted well with the formula: $\lambda^2 v$ = constant. With the increase in the growth rate, the hardness of the material decreases, the fracture toughness first increases and then decreases. The maximum hardness of the solidified eutectic ceramic rate reached 11.68 GPa when the solidification rate was 1 mm/h, this hardness was about 1.6 times that of the pre-sintered sample. Its maximum fracture toughness at room temperature was 7.21 MPa·m$^{1/2}$ when the rate was 3 mm/h, which was about two times that of the pre-sintered sample.

Keywords: $Al_2O_3/MgAl_2O_4/ZrO_2$, eutectic oxide ceramic, growth rate, induction zone melting, microstructure, fracture toughness

I. Introduction

More stringent requirements have been made for the new generation of ultra-high-temperature structural materials to meet demand for high-temperature structural materials in advanced aerospace applications, with the aim of saving energy and lessening any environmental impact. The new generation of ultra-high-temperature materials need to satisfy the following conditions [1]: (1) The temperature of the turbine inlet can reach or exceed 1700 °C; (2) the density of the material is less than 5.0 g/cm^3; (3) the material can be used long term in a harsh environment (such as a steam or humid environment); (4) cooling can be eliminated. However, the mainstream high-temperature structural material is single crystal superalloy, the maximum service temperature of which is only about 1100 °C while the density of the material is above 8 g/cm^3. Composites, such as C/C, SiC and Si_3N_4, cannot be used over a long time because they are easily oxidized when the temperature exceeds 1400 °C.

The eutectic self-forming composite material is formed by the matrix and reinforcing phase coexisting simultaneously from the melt in a directional solidification process. The necessary reinforcement fibers and the corresponding composite technology in traditional artificial composite materials are abandoned.The manmade interface between the matrix and the reinforcement phase is eliminated and the microstructure of the composite can be controlled by adjusting the parameters of the solidification process. For ceramic materials, the porosity and interface amorphous phases in the process of powder sintering are eliminated because of the directional solidification techniques. The density and deformability of the material increase. The sintered oxide ceramics are very sensitive to plastic deformation at high temperatures and cannot be used as a high-temperature structural material. However, the directionally solidified ceramics are becoming the preferred materials for long-term operation in high-temperature oxidizing atmosphere because of their excellent oxidation resistance at high temperature and corrosion resistance. Therefore, providing their mechanical properties can be improved at high temperatures, oxide ceramics are expected to become excellent ultra-high-temperature structural materials [2].

In 1969, Viechnicki *et al.* started research work on directionally solidified $Al_2O_3/Y_3Al_5O_{12}$ (YAG) eutectic ceramic [3]. In 1997, Waku *et al.* prepared YAG eutectic ceramic with the modified Bridgeman method [4,5]. During the past few years, the preparation and properties of oxide eutectic ceramics have attracted extensive attention from all over the world, and different rare-earth oxide eutectic ceramic systems have been investigated, including YAG [6], Al_2O_3/ZrO_2 [7], Al_2O_3/YAG/ZrO_2 [8], $Al_2O_3/GdAlO_3$ (GAP) [9] and Al_2O_3/Er_3AlO_{12}

* Corresponding author: jchliu@sdut.edu.cn

(EAG) [10]. Compared with rare-earth oxide eutectic ceramics, $Al_2O_3/MgAl_2O_4/ZrO_2$ eutectic ceramic has a great competitive advantage in terms of cost. Moreover, it has a high melting point of approximately 1830 °C, with high thermal conductivity and high toughness [11]. Therefore, in this work, oxide eutectic ceramics were prepared based on Al_2O_3, $MgAl_2O_4$ and ZrO_2.

However, research on the morphology, eutectic growth and solidification mechanism of $Al_2O_3/MgAl_2O_4/ZrO_2$ oxide eutectic ceramics has not received sufficient attention. Induction heating zone melting has the advantages of enabling a high melting temperature, a wide solidification rate range and the preparation of large samples. In this paper, the $Al_2O_3/MgAl_2O_4/ZrO_2$ oxide eutectic ceramics were prepared by means of induction heating zone melting. A large-size eutectic ceramic was obtained by means of controlled matching of high frequency power and the solidification rate. The effects of the solidification rate on the eutectic morphology, eutectic spacing and mechanical properties were investigated. The effect of the ZrO_2 phase size on the fracture toughness of the sample was discussed.

II. Experimental

Fig. 1 shows the $Al_2O_3/MgO/ZrO_2$ ternary eutectic phase diagram [12]. The specific composition and melting point are shown in Table 1 [12].

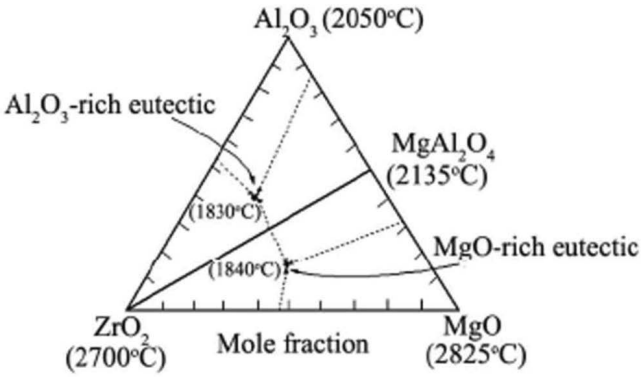

Fig. 1: Ternary $MgO/Al_2O_3/ZrO_2$ phase diagram.

Table 1: Compositions and melting temperatures of the two $Al_2O_3/MgO/ZrO_2$ ternary eutectics

	Al_2O_3		MgO		ZrO_2		Melting
	mol%	wt%	mol%	wt%	mol%	wt%	point/°C
Al_2O_3-rich	42.1	43	17.4	7	40.5	50	1830
MgO-rich	16.6	20	42.1	20	41.3	60	1840

The Al_2O_3-rich eutectic point with a melting point of 1830 °C in the equilibrium phase diagram was chosen in this study, where the mole ratio of Al_2O_3, MgO and ZrO_2 was 42.1:17.4:40.5 [12]. Commercial oxide powders (99.75 %, 5 μm) of Al_2O_3, MgO and ZrO_2 in the mole ratio of 42.1:17.4:40.5 were mixed homogeneously in a ball mill, with 5 % polyethylene water solution and a moderate amount of alcohol added as the mixing additive. Then the mixture was placed into a metal mold and a pressure of 20 MPa was exerted to form a precursor rod (∅ 10 mm × 20 mm) at room temperature. The rod was later sintered at 1550 °C for 2 h. The pre-sintered body was placed in a tungsten crucible in a high-frequency induction furnace, and the vacuum was maintained below 1×10^{-4} Pa with a molecular pump. The crucible was locally heated because the distribution of the induction magnetic field was not uniform under the action of high-frequency power. The sample in the parallel position of the coil was melted when the temperature of the crucible wall reached 2300 °C. The tungsten crucible descended with different rates of 1 mm/h, 2 mm/h, 3 mm/h and 5 mm/h respectively. Therefore, the coil scanned the crucible along its axis, a 2300 °C-high-temperature band scanned the rod with different rates, so that the rod melted and solidified step by step. The rate of magnitude of mm/h is small enough for the solidification rate to be almost identical to the crucible rate.

The microstructures of the samples were observed with scanning electron microscopy (SEM) equipped with an energy spectrum detector. The hardness and fracture toughness values of the samples were tested using a Vickers hardness tester at room temperature.

III. Results and Discussion

(1) Phase composition

Fig. 2 shows the XRD results of the pre-sintered body and the eutectic ceramic sample. As can be seen, the eutectic ceramic sample contains Al_2O_3 phase, $MgAl_2O_4$ phase and ZrO_2 phase, and more $MgAl_2O_4$ phase are formed after directional solidification.

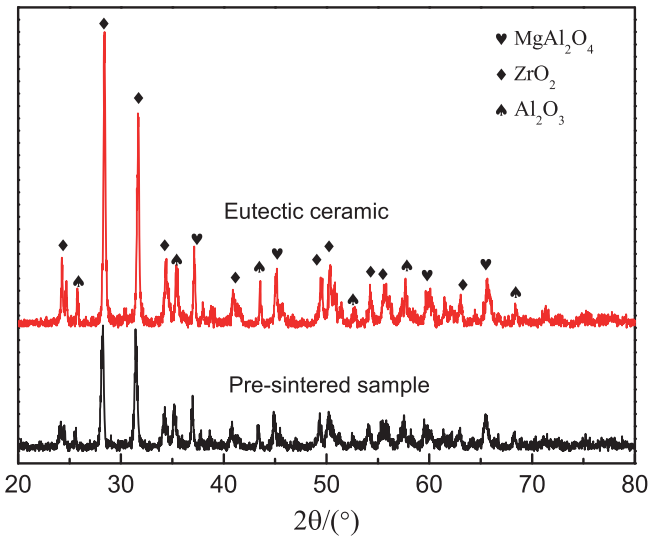

Fig. 2: XRD patterns of the pre-sintered ceramic and the eutectic ceramic.

Fig. 3 shows the SEM and EDS of the $Al_2O_3/MgAl_2O_4/ZrO_2$ eutectic ceramic. It can be seen that the $Al_2O_3/MgAl_2O_4/ZrO_2$ eutectic ceramic is composed of white and gray regions. The gray region contains Al, Mg and O elements, while the white region contains Zr and O elements. In combination with Fig. 2, it can be concluded that the gray region is composed of Al_2O_3 phase and $MgAl_2O_4$ phase, and that the white region corresponds to ZrO_2 phase.

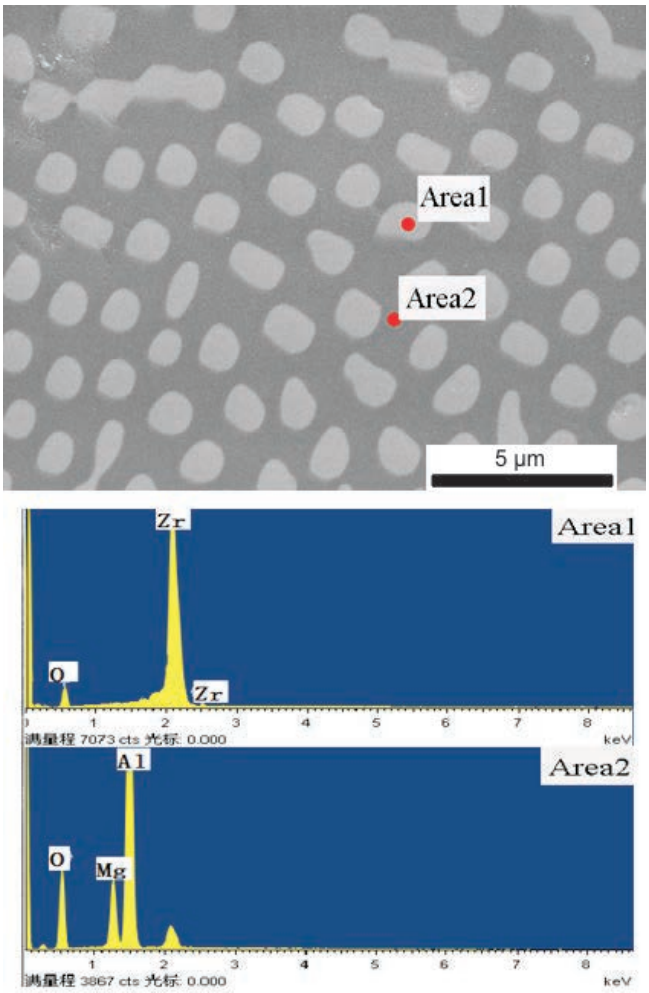

Fig. 3: Cross-section microstructure and EDS spectra of the solidified $Al_2O_3/MgAl_2O_4/ZrO_2$ ceramic (3 mm/h).

(2) Microstructure

Fig. 4 shows the cross-section microstructure of the unpolished sample, the longitudinal-section microstructure of the unpolished sample and the longitudinal-section microstructure of the polished sample when the growth rate is 3 mm/h. As can be seen, Al_2O_3 / $MgAl_2O_4$ constitute the matrix of the eutectic ceramic, while rod-like ZrO_2 phase is uniformly embedded in the matrix.

The Jackson factor is usually used to distinguish the faceted and non-faceted morphologies for different materials. It has two critical values, i.e. 2 and 5 [13]. Although the Jackson criterion is established under equilibrium solidification conditions, it can be used as a convenient criterion to predict the growth mode under normal solidification conditions. The calculation of the Jackson factor is based on the following equation:

$$\alpha = \frac{\varepsilon \Delta S}{R} = \frac{\varepsilon \Delta H}{RT_m} \qquad (1)$$

where ε is the crystallographic factor (less than but almost equal to 1), R is the gas constant, S is the entropy of fusion, H is the enthalpy of fusion, and T_m is the melting point of component phase. The entropies of fusion of Al_2O_3, $MgAl_2O_4$ and ZrO_2 are 5.74R [14], 9.82R [14] and 3.55R [14], respectively. According to Equation (1), $a_{Al_2O_3}$ = 5.74 and $a_{MgAl_2O_4}$ = 9.82, which are both greater than 5; a_{ZrO_2} = 3.55, which is between 2 and 5. Hence, Al_2O_3 and $MgAl_2O_4$ phases usually have smooth atomic interfaces and exhibit strong faceted growth characteristics, whereas the ZrO_2 phase presents either non-faceted or faceted morphology [15] and obeys the growth rules of a rod shape.

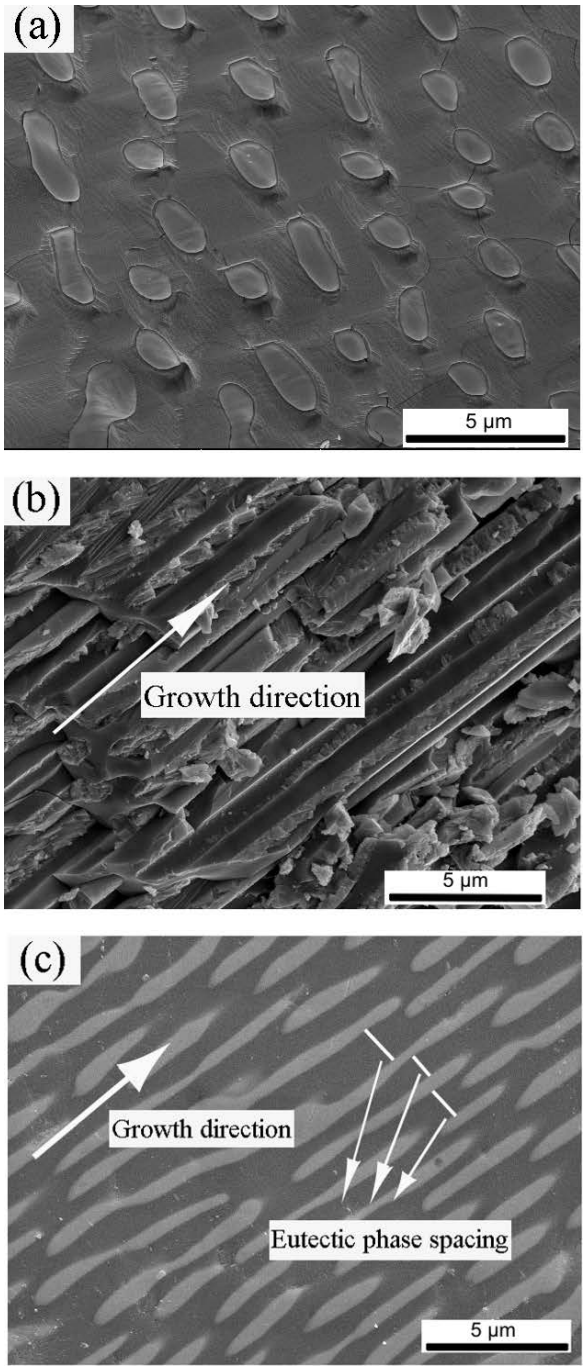

Fig. 4: SEM images of the $Al_2O_3/MgAl_2O_4/ZrO_2$ eutectic ceramic: (a) cross-section microstructure of the unpolished sample (3 mm/h), (b) longitudinal-section microstructure of the unpolished sample (3 mm/h), (c) longitudinal-section microstructure of the polished sample (3 mm/h).

Fig. 5 shows the cross-section microstructure of the eutectic ceramic at different growth rates. When the growth rate is less than 2 mm/h, Al_2O_3, $MgAl_2O_4$ and ZrO_2 phases show strong growth anisotropy of faceted planes, thus making the microstructure of the $Al_2O_3/MgAl_2O_4/ZrO_2$ eutectic ceramic present an irregular pattern as shown in Fig. 5(a) and Fig. 5(b). With the increase of the growth rate, the eutectic ceramic presents

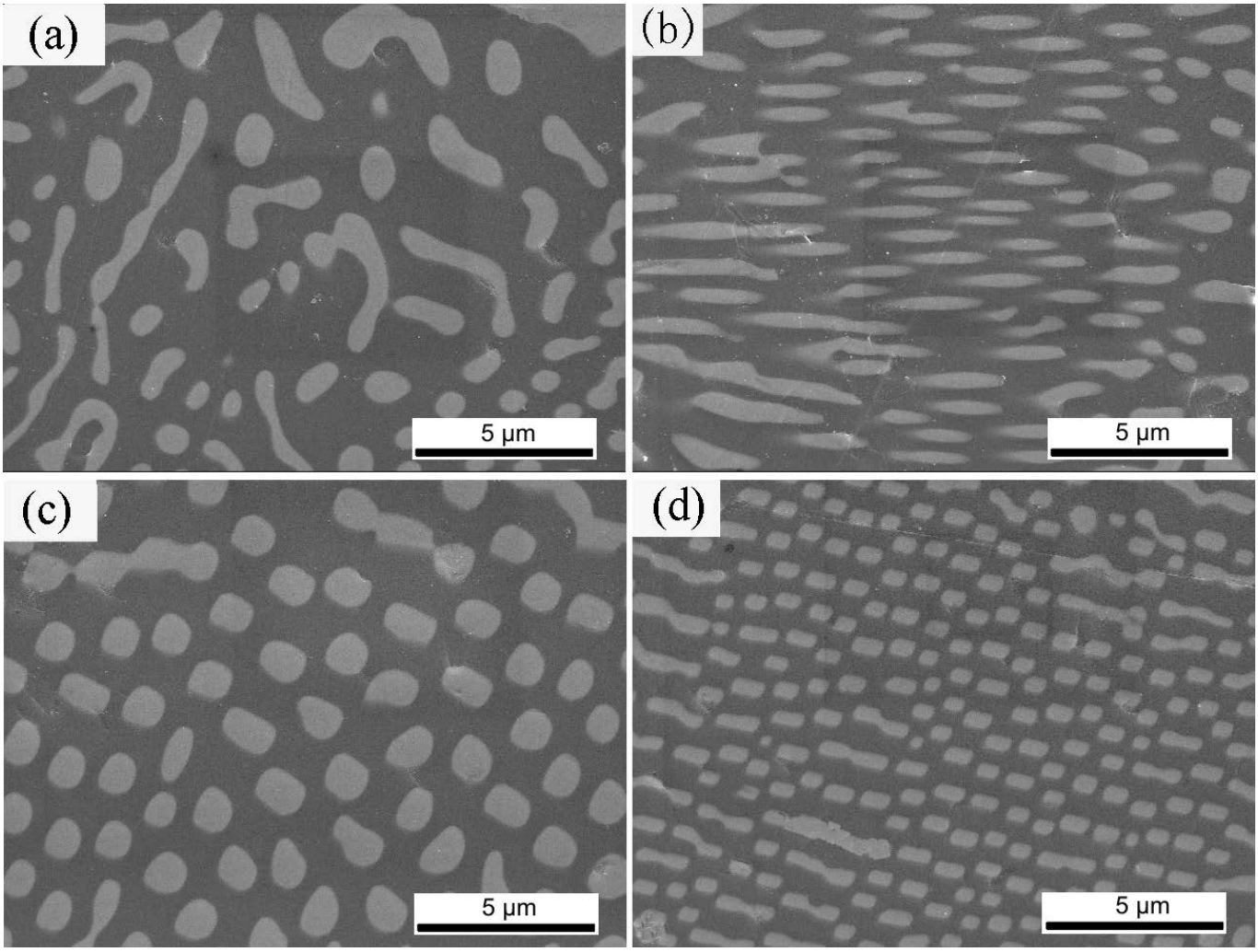

Fig. 5: Cross-section microstructure of the eutectic ceramic at different growth rates: (a) 1 mm/h, (b) 2 mm/h, (c) 3 mm/h and (d) 5 mm/h.

a layered and rod-like pattern as shown in Fig. 5(c). When the growth rate increases to 5 mm/h, as Fig. 5(d) shows, the eutectic ceramic presents a bar-shaped pattern. It is known that with a sufficiently high driving force (e.g. deep super cooling), the atomic interface of the phases even with high entropy of fusion may also become rough. In other words, the facets of the sample are converged to the non-facets. Therefore, the growth behavior of the eutectic ceramic tends to be more isotropic. Moreover, because of the positive correlation between the super cooling and the growth rate, a further increase of the growth rate to 3 mm/h can produce a layered and rod-like microstructure pattern as shown in Fig. 5(c); when the growth rate increases to 5 mm/h, the microstructure presents a more regular bar-like pattern as shown in Fig. 5(d).

Fig. 4(c) shows the eutectic phase spacing. Fig. 6 shows the relationship between the average eutectic phase spacing and the growth rate. The test result shows that $\lambda^2 v = 2.98$. Although the microstructure of the eutectic ceramic presents a complex regular structure, it still meets the J-H theory and the eutectic spacing decreases gradually with the increase in the growth rate. Moreover, the microstructure is finer than that of the eutectics with rare earth oxides. This can be attributed to the higher temperature gradient and relatively fast solidification rate. Meanwhile, the large volume fraction of ZrO_2 is very important for the refinement of the microstructure.

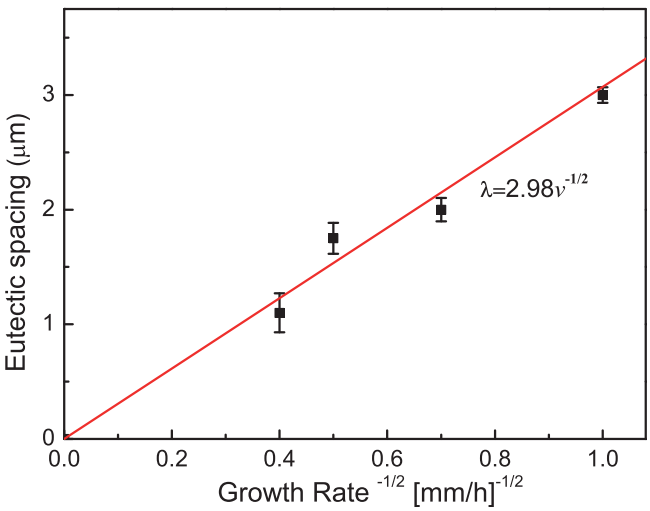

Fig. 6: Dependence of the average eutectic phase spacing on the growth rate.

(3) Mechanical properties

The hardness of the eutectic ceramic was tested using the Vickers indentation technique with a load of 9.8 N for 15 s,

and the fracture toughness was calculated on the basis of the measured hardness using formula (2) [16]. The diamond indenter with proper pressure can produce indentation and a crack along the indentation diagonal. As shown in Fig. 7, the length of the indentation diagonal is 2*a* and that of the crack is *l*; $c = l + a$. Fig. 8 shows the Vickers indentation morphology of $Al_2O_3/MgAl_2O_4/ZrO_2$ eutectic ceramic. In the process of the experiment, the load of 9.8 N was not enough to produce the median crack ($c/a > 2.5$), and the crack was produced until the load reached 49 N.

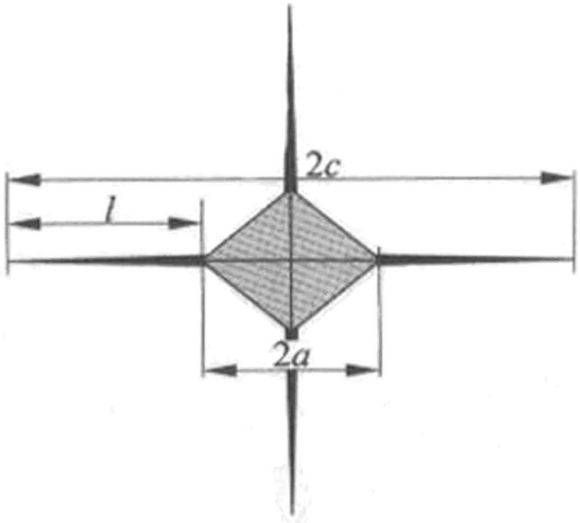

Fig. 7: Vickers micro-indentation schematic diagram.

$$K_{IC} = 0.016 \left(\frac{E}{H_V}\right)^{\frac{1}{2}} P c^{-\frac{2}{3}} \quad (2)$$

where E is the material elasticity modulus (GPa), H_V is the Vickers hardness (GPa), K_{IC} is the fracture toughness (MPa·m$^{1/2}$), P is the indentation load, and c is the indentation crack length.

Table 2 gives the hardness and fracture toughness of the pre-sintered ceramic and the ZM eutectic ceramic. The results show that there is little difference in the hardness and fracture toughness of the cross- and longitudinal sections of the eutectic ceramic; the hardness and fracture toughness of the eutectic ceramic are much higher than those of the sintered ceramic with the same composition, the maximum hardness of the eutectic ceramic reaches 11.68 GPa, which is 1.6 times that of the sintered ceramic; the maximum fracture toughness is 7.21 MPa·m$^{1/2}$, which is two times that of the sintered ceramic. The main reasons for the increase in hardness and fracture toughness of the eutectic ceramic include the densification of the microstructure, the disappearance of pores and grain boundaries, and the distribution of the finer ZrO_2 phase in the Al_2O_3 and $MgAl_2O_4$ matrix. In Fig. 8(b), parallel cracks can be seen, and the principal crack is accompanied by several microcracks. In Fig. 8(c), crack deflection and bifurcation can be seen, and these behaviors can deplete the energy of crack growth and expansion, thus improving the fracture toughness of the material. In addition, it can be observed that some cracks appear along the layer in this sample in Fig. 8(d). Residual thermal stress should appear in the matrix phase because the ZrO_2 phase existed, and the ZrO_2 phase played a role in stress toughening.

Fig. 9 shows the relationship between the cross-sectional hardness and fracture toughness of the eutectic ceramic and the growth rate. As can be seen, with the increase in the growth rate, the hardness of the material decreases while the fracture toughness first increases and then decreases.

The toughening mechanism of the ZrO_2 phase is that the phase transformation of *t-m* appears when it is subjected to stress, a lot of energies are absorbed because of the volumetric and shape effects produced by phase transformation, and hence the material exhibits high toughness. However, the toughening action of ZrO_2 phase is affected by the size of the ZrO_2 phase, *d*. At room temperature, there is a critical phase size d_c (about 0.64 μm [17]), an upper critical size, the ZrO_2 phase is likely to produce phase transformation toughening only if the ZrO_2 phase size is less than the critical phase size, i.e., $d < d_c$. There is another critical diameter d_I (about 0.42 μm [17]), a lower critical size that the ZrO_2 phase must exceed if it is to effect phase transformation toughening. In other words, when $d_I < d < d_c$, stress would induce ZrO_2 phase *t-m* transformation, which toughens the material containing the ZrO_2 phase.

During the cooling process from high temperature to low temperature, ZrO_2 converts into *m* phase if $d > d_c$, from which phase transformation would induce micro-cracks or residual stress in the material owing to the volume effect, just as the experimental results had shown. The third

Table 2: Hardness and fracture toughness of the pre-sintered ceramic and the ZM eutectic ceramic.

Properties		Pre-sintered ceramic	Solidified ceramic			
			1 mm/h	2 mm/h	3 mm/h	5 mm/h
Hardness (GPa)	Cross section	7.2	11.68	10.40	9.37	8.92
	Longitudinal section		10.32	10.77	8.56	8.38
Fracture toughness (MPa·m$^{1/2}$)	Cross section	3.5	6.24	6.57	7.21	5.13
	Longitudinal section		6.55	6.39	7.39	5.24

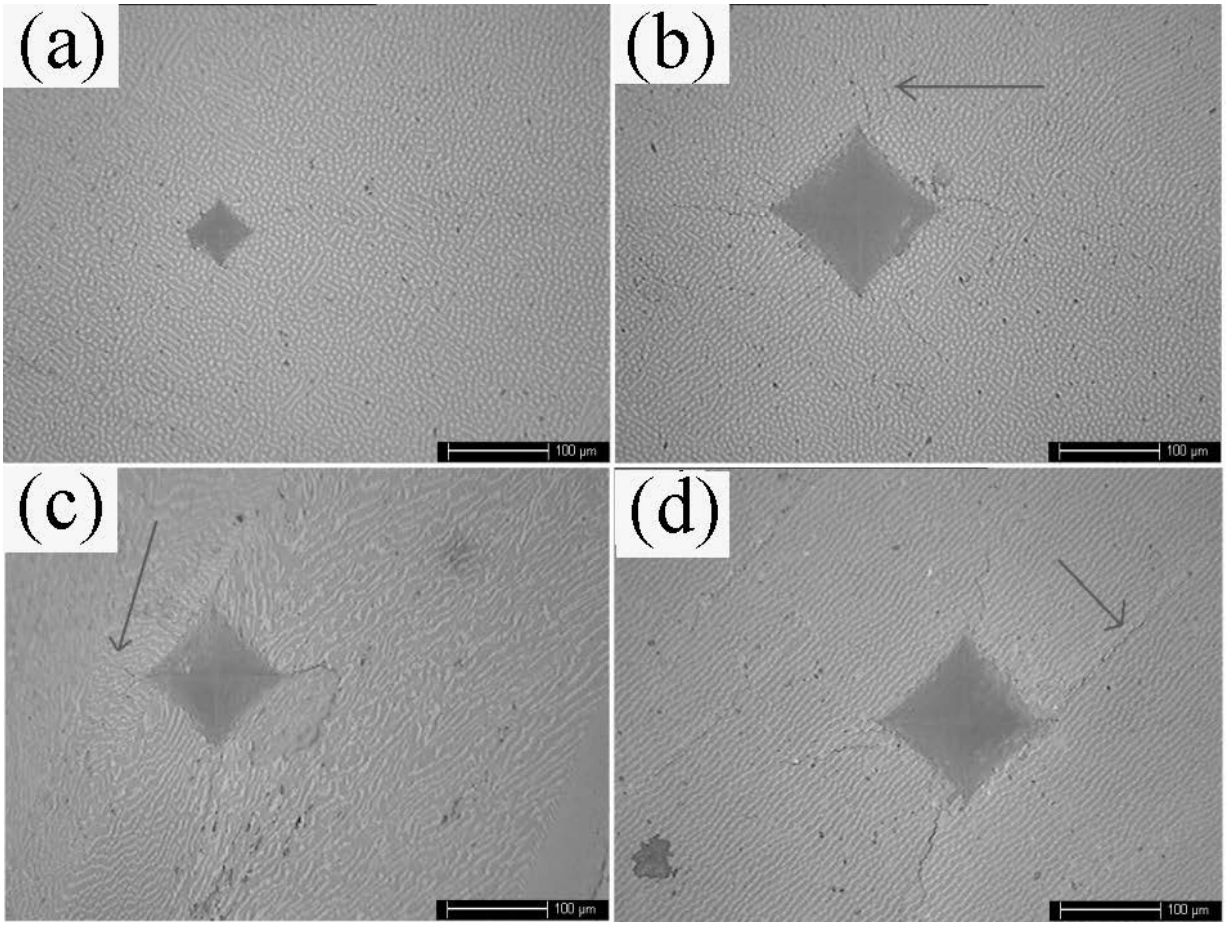

Fig. 8: Vickers indentation morphology of $Al_2O_3/MgAl_2O_4/ZrO_2$: (a) indentation morphology with the load of 9.8 N, the load of 9.8 N was not enough to produce the median crack, and the crack was produced until the load reached 49 N, (b) cross-section indentation morphology with the load of 49 N, (c) and (d) longitudinal-section indentation morphology with the load of 49 N.

critical size, d_m (about 0.83 μm [17]), appears. When $d > d_m$, ZrO_2 phase transformation during the cooling process induces micro-cracks; and $d_c < d < d_m$, the phase transformation cannot induce micro-cracks, but results in residual stress around it. Both micro-cracks and residual stress effect a toughening. The above theory is based on polycrystalline sintered ceramics with nearly equiaxed grains. With the help of this theory, we try to explain the mechanical properties of this single crystal multiphase solidification ceramic herein.

It can be seen from Fig. 5 that the size of the ZrO_2 phase decreases with the increase in the solidification rate. In Fig. 5(a) and 5(b), the average size of the ZrO_2 phase is larger (1.2 μm and 0.94 μm only from cross-section, respectively; much larger from a three-dimensional view, see Fig. 5), i.e. $d > d_m > d_c$, ZrO_2 is *m* phase at room temperature, the residual stress of phase transformation leads to micro-cracking toughening. The micro-crack density increases with the decrease in the ZrO_2 phase size, and the micro-cracking toughening becomes enhanced.

In Fig. 5 (c), the average size of ZrO_2 phase is 0.72 μm from the cross-section, about 5 μm from the longitudinal section. None of these sizes satisfies the condition, $d_I < d < d_c$. However, we suppose that the upper critical size for ZrO_2 phase transformation for this single crystal multiphase solidification ceramic, $d_{c\text{-}s}$, might be rather larger than that for polycrystalline sintered ceramic, d_c. Therefore, the further improvement in the solidified ceramic could be attributed to the phase transformation toughening as the solidification rate increases from 2 to 3 mm/h.

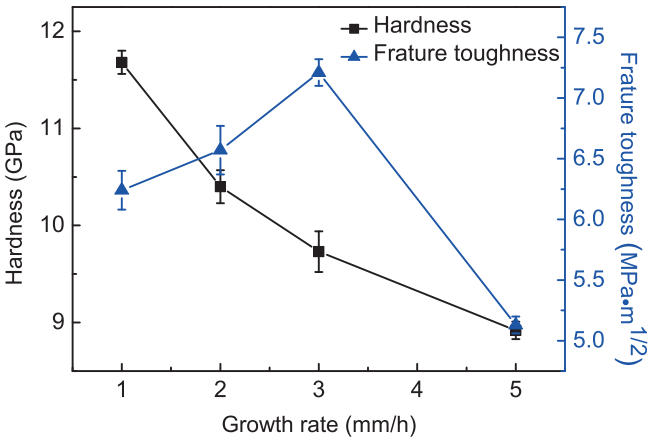

Fig. 9: Dependence of cross-section hardness and fracture toughness on the growth rate.

As shown in Fig. 5 (d), the phase average size is 0.37 μm, $d < d_I$, the stability of *t* phase increases, *t-m* phase transformation is blocked. Either phase transformation toughening or micro-cracking toughening, even residual stress toughening significantly is reduced, so the toughness of the material decreases.

The bond hardness ($H_{a\text{-}b}$) is the hardness average of the bond atoms assigned to the *a-b* bond; it represents the chemical bond ability to capture electrons in unit volume. The relationship between the bond hardness and the hardness is:

$$H = 423.8\, H_{a-b} - 3.4 \quad (3)$$

Super cooling degree and solidification rate are positively correlated. As the solidification rate increases, both the super cooling degree and the melt viscosity increase. The ability of the chemical bond to capture electrons per unit volume declines with the decline of the electron diffusion ability in the melt. Hence the hardness of material decreases.

When the solidification rate is 1 mm/h or 2 mm/h, the ZrO_2 phase size is larger than d_m, and the residual stress formed in the cooling process is large enough to cause micro-cracks, which weaken the binding capacity between the phases. As the micro-crack density increases with the decrease of ZrO_2 phase size, the material hardness decreases.

When the solidification rate is 3 mm/h, the super cooling degree increases, and more high temperature ZrO_2 *t* phase is retained to room temperature, the hardness decreases with the increase of the amounts of *t-m* phase transformation [18].

The relationship between the residual stress and the hardness is:

$$H|_ = a_1 (\sigma / \sigma)^2 + a_2 (\sigma / \sigma) + a_3 \quad (4)$$

where $H|_p$ is the hardness of the material, a_1, a_2 and a_3 are quadratic polynomial coefficients, σ_{res} is the residual stress, σ_y is yield stress. The hardness of the material decreases with the decrease in the residual stress. When the solidification rate is 5 mm/h, the residual stress in the material is gradually eliminated, so the hardness of the material decreases.

Considering the effects of growth rate on the microstructure and mechanical properties, good directionally solidified eutectic ceramic with better performance and finer microstructure can be obtained at the growth rate between the 2 ~ 3 mm/h. The hardness of the material is lower than that of rare-earth garnet series but higher than that of commonly sintered samples (Table 2), and its fracture toughness is slightly higher than that of ceramics reported by Zhang and others [16, 19].

IV. Conclusions

Smooth $Al_2O_3/MgAl_2O_4/ZrO_2$ eutectic ceramic rods were prepared with induction heating zone melting and the effects of the growth rate on the microstructure and properties of the solidified ceramic were investigated.

(1) The $Al_2O_3/MgAl_2O_4/ZrO_2$ eutectic ceramic is composed of Al_2O_3 phase, $MgAl_2O_4$ phase and ZrO_2 phase. It has a typical layered and rod-shaped eutectic structure, and the eutectic spacing is very fine. The eutectic spacing λ, and solidification rate v, conform to the following formula: $\lambda^2 v = 2.98$.

(2) As the solidification rate increased, the specimen morphology transformed from an irregular morphology to a regular layered or rod-like structure. The fracture toughness increased first and then decreased owing to the toughening effect of ZrO_2 phase, which was affected by the size of the ZrO_2 phase.

(3) The maximum hardness of the solidified eutectic ceramic rate reached 11.68 GPa when the solidification rate was 1 mm/h, which was about 1.6 times that of the pre-sintered sample. Its maximum fracture toughness at room temperature was 7.21 MPa·m$^{1/2}$ when the rate was 3 mm/h, which was about two times that of the pre-sintered sample.

Acknowledgment

This work was financially supported by the Natural Science Foundation of China (NSFC, Grant No. 51172161), and Natural Science Foundation of Shandong Province (Grant No. ZR2012EMM018).

References

1 Otuska, D., Waku, Y., Kitagawa, K., Arai, N.: Effect of hot corrosive environment on ceramics, *Energy*., **30**, 523 – 533, (2005).

2 Stubican, V.S., Bradt, R.C.: Eutectic solidification in ceramic systems, *Ann. Rev. Mater. Sci.*, **11**, [1], 267 – 297, (1981).

3 Viechnicki, D., Schmid, F.: Investigation of the eutectic point in the system Al_2O_3-$Y_3Al_5O_{12}$, *Mater. Res. Bull.,* **4**, 129 – 135, (1969).

4 Waku, Y., Nakagawa, N., Wakamoto, T.: A ductile ceramic eutectic composite with high strength at 1873 K, *Nature.,* **389**, 49, (1997).

5 Waku, Y.: A new ceramic eutectic composite with high strength at 1873 K, *Adv. Mater.,* **10**, 615 – 617, (1998).

6 Pastor, J.Y., LLorca, J., Salazar, A.: Mechanical properties of melt-grown Alumina-Yttrium aluminum garnet eutectics up to 1900 K, *J. Am. Ceram. Soc.,* **88**, 1488 – 1498, (2005).

7 Song, T.T.: Microstructure and mechanical properties of Al_2O_3/ZrO_2 directionally solidified eutectic ceramic prepared by laser 3D printing, *J. Mater. Sci. Technol.,* **32**, 320 – 325, (2016).

8 Song, K., Zhang, J., Lin, X.: Microstructure and mechanical properties of $Al_2O_3/Y_3Al_5O_{12}/ZrO_2$ hypereutectic directionally solidified ceramic prepared by laser floating zone, *J. Eur. Ceram. Soc.,* **34**, 3051 – 3059, (2014).

9 Ohashi, Y., Yasui, N., Suzuki, T.: Orientation relationships of unidirectionally aligned $GdAlO_3/Al_2O_3$ eutectic fibers, *J. Eur. Ceram. Soc.,* **34**, 3849 – 3857, (2014).

10 Mesa, M.C., Oliete, P.B., Orera, V.M.: Microstructure and mechanical properties of $Al_2O_3/Er_3Al_5O_{12}$ eutectic rods grown by the laser-heated floating zone method, *J. Eur. Ceram. Soc.,* **31**, 1241 – 1250, (2011).

11 Zhai, S., Liu, J.C., Wang, J.: Microstructure of the directionally solidified ternary eutectic ceramic $Al_2O_3/MgAl_2O_4/ZrO_2$, *Ceram. Int.,* **42**, 8079 – 8084, (2016).

12 McKittricka, J., Kalonjib, G.: Non-stoichiometry and defect structures in rapidly solidified MgO-Al_2O_3-ZrO_2 ternary eutectics, *Mat. Sci. Eng.*, **A231**, 90 – 97, (1997).

13 Jackson, K.A.: Constitutional supercooling surface roughening, *J. Cryst. Growth,* **264**, 519 – 529, (2004).

14 Su, H.J., Zhang, J., Liu, L., Fu, F.H.: Processing and microstructure of Al_2O_3/YAG eutectic ceramic by laser rapid remelting, *J. B. Univ. Aeronaut. Astronaut.*, **33**, [7], 846 – 850, (2007).

15 Pastor, J.Y., Llorca, J., Poza, P.: Mechanical properties of melt-grown Al_2O_3–ZrO_2 (Y_2O_3) eutectics with different microstructure, *J. Eur. Ceram. Soc.,* **25**, 1215 – 1223, (2005).

16 Deng, Y.F., Zhang, J., Su, H.J.: Microstructure and fracture toughness of $Al_2O_3/Er_3Al_5O_{12}$ eutectic ceramic prepared by laser zone remelting, *J. Inorg. Mater.,* **26**, 841 – 846, (2011).

[17] Ge, Q.L., Zhou, Y., Lei, Y.Q.: Study on microstructure and properties of ZrO_2-2 mol% Y_2O_3 ceramics, in chinese, *J. Chin. Ceram. Soc.,* **1**, 47 – 53, (1990).

[18] Yashima, M., Kakihana, M., Yoshimura, M.: Metastable-stable phase diagrams in the zirconia-containing systems utilized in solid-oxide fuel cell application, *Solid State Ionics,* **86 – 88**, [96], 1131 – 1149, (1996).

[19] Su, H., Zhang, J., Cui, C.: Growth characteristic of Al_2O_3/$Y_3Al_5O_{12}$ (YAG) eutectic ceramic *in situ* composites by laser rapid solidification, *J. Alloy. Compd.,* **456**, 518 – 523, (2008).